Mechanisms of Axonal Injury: an Experimental and Numerical Study of a Sheep Model of Head Impact

RWG Anderson[1], CJ Brown[2], PC Blumbergs[3], G Scott[3], JW Finney[3], NR Jones[2], AJ McLean[1]

[1]Road Accident Research Unit, University of Adelaide,
[2]Department of Surgery (Neurosurgery), University of Adelaide
[3]Division of Tissue Pathology, Institute of Medical and Veterinary Science

ABSTRACT

This paper investigates the relationship between the incidence of axonal injury and the tissue mechanics produced by an impact to the head in an animal model. The data are drawn from an experimental model of brain injury using sheep where the dynamics of the head impact are measured. Measurements include impact force, head acceleration and subdural pressures. A preliminary finite element model of the sheep skull and brain is presented. Simulations of selected experiments are used to estimate mechanics of the brain tissue during the impact. The resulting injury in the brain tissue was mapped using amyloid precursor protein as a marker for injury. A comparison is made between the von Mises' stresses predicted by the finite element model, and the incidence of injury in various regions of the brain. The results of the model suggest that a trend exists between high levels of stress and the incidence of injury. All experiments conformed to the Australian Code of Practice for the Care and Use of Animals for Scientific Purposes.

THE INVESTIGATION OF BRAIN INJURY MECHANISMS remains a crucial part of formulating criteria for the assessment of head injury risk. Despite many years of work, there is still no general agreement on a well founded method of determining the risk of injury to the human brain due to blunt impact to the head. Studying the biomechanics of brain injuries such as axonal injury in living animals can provide important insights into the mechanisms of injury. In a well defined animal model, it should be possible to relate the incidence of injury in the brain tissue of the animal to the output of a numerical model of the experiment. Such an analysis should provide a threshold of stress or strain above which injury is likely to occur. The threshold for injury may apply across species. If so, then the value of the threshold determined from such an experimental approach may be directly applied to numerical models of impact to the human head. The analysis of such models would be able to estimate the risk of injury for a given impact.

The validity of numerical techniques for modelling head impact can also be examined using this experimental approach. For example, different interface conditions between the skull and the brain can be applied to the model to examine their effects on the results of the model. Similarly, the inclusion of anatomical details can be investigated to determine how much detail is required in a numerical model to be able to correctly predict the dynamics of the brain in an impact.

In this paper we report on results of work which is designed to investigate the mechanisms of axonal injury produced by an impact in a sheep model of head injury. The paper describes new techniques for validating acceleration measurements, and techniques for controlling coordinate data. These techniques have improved our confidence in the acceleration measurements over those made in previous experiments (Anderson et al., 1997). We also present a preliminary finite element model, which is used to investigate injury thresholds in the animal model.

AIMS

The aims of this study were to:

- Characterise head impacts in an animal model of axonal injury
- Relate the incidence of injury to a preliminary finite element model of the impact.

METHODS

OVERVIEW - This study is comprised of several stages; they were

- the animal experiment which incorporated the biomechanical measurements,
- the application of the measured head dynamics to a finite element model of the experiment,
- the recording of the injury resulting from the impact, and
- a correlation between the observed injury and the output of the finite element model.

The biomechanics of the experiment were measured in a manner that allowed the dynamics to be accurately reproduced in the finite element model. The biomechanics of the impact were characterised by the linear and angular acceleration of the head about a defined set of axes, the impact force, the impact velocity, and the pressure in the cerebrospinal fluid at defined locations. The force and acceleration measurements were applied to a finite element model of the sheep's skull and brain and the pressure measurements were used to validate the output of the finite element model.

The axonal injury in each animal was recorded by taking coronal sections of the brain and applying histological techniques to identify the injury. To compare the results of the finite element model to the injury produced in the model, we needed to be able to identify the location of the coronal section in the model. This was made possible by producing magnetic resonance imaging (MRI) data and computed tomography (CT) data of the head of a single animal. These data consisted of geometrical information of the entire volume of the brain. These data were transformed so that the geometry of the head in each set of data was exactly aligned. The CT data was used as a basis for the finite element model and the MRI data was used to identify the location of each histology section (The MRI data contained finer anatomical details of the brain). Because the CT and MRI data were aligned, results data from the finite element model could be extracted on the same plane as the histology section.

The success of interchanging data between different stages of the study hinged on measuring coordinate data. In the experiments, measurements were made of the position and orientation of the striker and of all instrumentation on the head. These measurements were made in relation to anatomical features on the sheep's head. These anatomical features were also identified in the medical imaging data. This facilitated the application of the force and acceleration to the finite element model.

ANIMAL PREPARATION - All experiments conformed to the Australian Code of Practice for the Care and Use of Animals for Scientific Purposes (National Health and Medical Research Council, 1997). The animal was anaesthetised with diazepam (1 mg/

kg) and ketamine (4 mg/kg). The animal was then intubated and mechanically ventilated under isofluorane (2 per cent), until a ketamine intravenous line was established. Anaesthesia was maintained by an intravenous infusion of a ketamine/saline solution (15 mg/kg/hr) and isofluorane (1 per cent). The animal was ventilated with 100 per cent oxygen (3 l/min) until blood gases could be verified. Blood gas samples were then taken at 10 minute intervals for the duration of the experiment. Ventilation was adjusted to maintain $PaCO_2$ at 40 mmHg and PaO_2 at 110 ± 10 mmHg (core temperature corrected values). Other physiological parameters that were monitored and digitally recorded throughout the experiment were central venous pressure (CVP), arterial blood pressure (ABP), sagittal plane electrocardiogram (ECG), intracranial pressure (ICP), core temperature and fluid balance.

Once the animal had been instrumented for physiological measurements, biomechanical sensors were attached

ACCELEROMETER ARRAY - We have previously reported on an accelerometer array used to measure the head kinematics in this animal model (Anderson et al., 1997). The major source of error with the first array was found to be the presence of relative motion between the skull and the array. The design of an improved array (Figure 1) has several advantages over the previous design:

- the array attaches directly to the skull, eliminating the need for the attachment plate used in the first design
- spacers are not required, thereby eliminating a source of relative motion
- better attachment techniques are used
- the accelerometers are placed nearer to the attachment points, minimising the effects of any relative motion
- the array has a tenth accelerometer which is a 'floating' member of the array. This accelerometer is attached to the skull and acts as a reference, providing an independent measure of the validity of the acceleration measurement in each experiment.

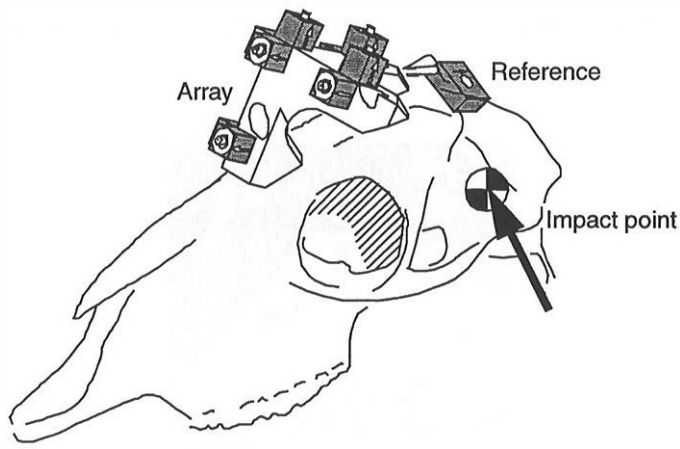

FIGURE 1. 3-2-2-2 array in position on the skull of the sheep

If the acceleration of a rigid body is known, the acceleration at any known point on the rigid body can be calculated. This is the basis of the reference accelerometer concept. An accelerometer placed on the skull recorded the acceleration experienced by a single point on the head during the impact. The output of the array was used to predict the appropriate component of acceleration of the rigid body at that point. The cross correlation between the prediction of the array, and the acceleration measured by the

reference accelerometer was computed. The cross correlation provides a statistical measure of the reliability of the acceleration measurement in any given experiment.

A poor correlation may be a result of poor attachment of either the array or the reference. But if the predicted and measured acceleration correlate well, one can have a certain confidence that the array successfully measured the rigid body motion of the skull. This technique is useful in animal experiments because the ability of the array to measure the rigid body motion of the skull must be validated during the experiment itself; the quality of the attachment cannot be characterised generally.

The array was held in place with four orthopaedic self tapping screws; one near each horn bud at the rear of the array, and two above the distal end of the frontal bone, above the olfactory sinus. The array attachment points were chosen to sit above air sinuses in the sheep skull. Before attachment, and after the animal was anaesthetised and ventilated, a pneumatic surgical burr was used to open up the air sinus. A fast setting epoxy putty was forced into the sinus, forming a wedge and an anchor for the screws. Putty was added to provide adequate seating for the feet of the array. Once the putty had set, holes were drilled and tapped and the array was attached.

The reference accelerometer was attached to the posterior face of the right horn bud, roughly aligned with the direction of the impact. The aim was to measure a significant component of the acceleration of that region of the skull. The putty placed in the air sinus on the right side of the skull also provided an anchor for the screw that held the reference array in position.

DYNAMIC INTRACRANIAL PRESSURE MEASUREMENTS - The anatomy of the head of the sheep allows only a limited number of locations to be selected for the pressure measurements at the surface of the brain; only regions where the bones of the cranium are near the surface of the skin are accessible for mounting the devices.

Two locations were selected. One location was on the left of the midline of the brain, near the impact point, and the other was located on the right of the midline, toward the *contrecoup* region of the brain (Figure 2). The locations of the pressure transducers were arbitrary and chosen with regard to other instrumentation that was mounted on the skull. The exact location of each transducer was measured relative to the anatomy of the skull using a three dimensional coordinate measuring arm (Microscribe-3DX, Immersion Corporation).

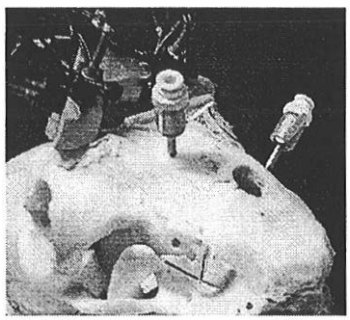

FIGURE 2. Typical pressure transducer locations

The transducers were Endevco 8514 pressure transducers with a range of 0 - 50 psi (0 - 345 kPa) that had been doped to resist slightly saline solutions. They were mounted using modified Camino intracranial pressure monitor bolts. The bolts are hollow and the sensor is inserted so that the tip of the sensor is flush with the end of the bolt. A collet, silicon ring and hollow nut provide a pressure seal. Holes, three millimetres in diameter, were drilled through the skull to the surface of the dura, and micro-operating

tools were used to cut and remove the dura directly underneath the hole. The lower edge of the hole was cleaned of any remaining bone, and any bone fragments were removed. Removal of the dura allowed the tip of the transducer to be in contact with the cerebrospinal fluid. The bolts were flushed with sterile saline before the pressure transducers were inserted with the aim of removing any air between the transducer and the cerebrospinal fluid.

IMPACT DEVICE - The impact to the sheep's head was delivered by a modified Schermer MKL captive bolt gun. Our previous communication describes the mechanics and operation of the gun (Anderson et al., 1997). The striker's mass is 395 g and the impact velocity can be varied up to 40 m/s. Typically, the measured impact force ranges between 5 and 8 kN over durations of 2 to 3 ms.

COORDINATE SYSTEM CONTROL - Multiple reference frames provided a means of relating the results from one phase of the study to the next. More specifically, loading measured in the experiment had to be applied to the finite element model and finite element model predictions needed to be related to locations of injury in the brain. The complex motion of the head and the three dimensional representation of the brain in the finite element model complicate this process. An anatomical coordinate system was the basis for recording coordinate data in this study. The coordinate system uses the point of bregma on the exterior of the skull and the two infraorbital notches on the zygomatic processes to define an anatomical coordinate system. This coordinate system could be identified during the surgical procedure on the living sheep, on the post mortem skull, and in the medical imaging data used to construct the finite element model (CT and MRI data). It was also indirectly accessible in the neuropathology data by identifying the cutting plane of the histology section in the MRI data.

A three dimensional coordinate measuring arm was used to relate physical coordinate systems to the anatomical coordinate system. Using the arm, coordinate transformation parameters were defined between any pertinent coordinate system and the positions of instrumentation; namely the array, the reference accelerometer and the pressure transducers. The impact point and the impact direction could also be related to the anatomical reference system. These positions could then be transformed to the coordinate system of the finite element model for application to the model. Figure 3 illustrates the typical coordinate system and instrumentation layout in a given experiment.

KINEMATIC MEASUREMENTS - All kinematic data was collected using a high speed digital acquisition system. Acceleration, force and pressure measurements were filtered with a 10 kHz analogue filter and subsequently filtered with a digital 4th order 3 kHz elliptical filter. Linear and angular acceleration were calculated in the manner described by Padgaonkar et al. (1975) and corrected where necessary by the methods described in Plank et al. (1989). The kinematics of the experiment was recorded using a high speed cine camera (1000 frames per second).

NEUROPATHOLOGY - After the impact, the animal continued to be monitored and supported physiologically for a further four hours. At the end of the survival period the animal was sacrificed using a perfusion of 4% paraformaldehyde which also fixed the brain tissue. The cranial cavity was opened using a craniotome, the dura was cut and the brain was removed intact. The brain was placed in a bath of the paraformaldehyde solution for a minimum period of one week to ensure complete fixation of the tissue.

Following fixation, the brain was sectioned in the coronal plane at 5 mm intervals. Each section was embedded in paraffin wax and histology sections were cut from each block and mounted on microscope slides. The mounted tissue was stained for the presence of amyloid precursor protein (APP), a reliable marker of axonal injury (Gentleman et al., 1993).

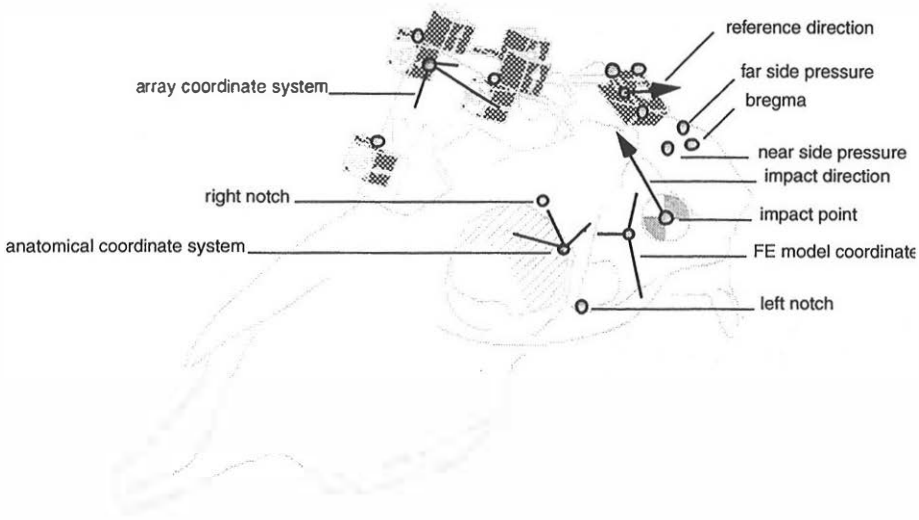

FIGURE 3. Coordinate system layout in experiment 0198

Each section was examined by placing a 4mm grid over the section. The grid provided a means of quantifying and describing the distribution of injury. A grading system (Table 1) was used in conjunction with the grid to map the distribution and the severity of the injury.

Table 1: Grading system for mapping axonal injury

Number of injured axons per 4x4 mm square	Injury grade
1 - 10	1+
>10	2+
stain visible macroscopically	3+

EXPERIMENTAL RESULTS

MACROSCOPIC PATHOLOGY - In experiments in which there was no skull fracture, the brain of the animal often exhibited mild subarachnoid haemorrhage and isolated petichial haemorrhages in the cortex. In two experiments there was a linear fracture at the impact point. The macroscopic features of the pathology in these cases included patchy subarachnoid haemorrhage and, in one case, a contusion under the impact point (Experiment 0498). The contusion extended through the thickness of the cortex. Depressed fractures produced significant cortical contusions and associated subarachnoid haemorrhage. Often the contusions extended beyond the cortex and into the digitate white matter of the left hemisphere. In some cases of severe comminuted fracture, the brain tissue was lacerated at the site of the contusion. In several cases the subarachnoid haemorrhage was present around the brain stem and the base of the brain.

MICROSCOPIC PATHOLOGY - The brains of all animals contained widespread axonal injury of a severity of 1+. There was extensive 2+ injury in the mid-brain, along the margins of the lateral ventricles, and in tissue surrounding impact contusions. There was also 2+ injury to a lesser extent in some of the digitate white matter of the cortex.

BIOMECHANICS - A summary of the results is presented in Table 2. Cross correlation coefficients between the reference accelerometer and the array predictions provide a measure of the validity of the acceleration measurements. Excluding

experiment number 0997, which had a poor cross correlation coefficient, the angular acceleration of the sheep heads were in the range of 97 to 199 krad.s^{-2}.

Table 3 summarises the peak pressures (relative to atmospheric pressure) measured at the surface of the brain in the experiments. Pressure measurements were clipped in the first few experiments and only indications of their magnitude can be given here (indicated by the ">" sign).

Table 2: Summary of rigid body dynamic results

Experiment	Impact velocity (m.s^{-1})	Maximum force (kN)	Maximum linear acceleration of the head[a] (km.s^{-2})	Maximum angular acceleration of the head (krad.s^{-2})	ρ_0, ρ_{max} [b]
0697	44.6	10.0	14.3	189	n.a.
0797	44.6	5.4	10.1	111	n.a.
0897	45.2	5.5	13.1	196	0.81, 0.91
0997	42.0	8.1	15.9	300	0.57, 0.88
1097	42.0	10.8	14.8	165	0.92, 0.92
0198	32.5	6.4	10.4	143	n.a.
0298	28.6	7.0	16.9	199	0.86, 0.89
0398	23.0	5.7	9.7	143	0.95, 0.98
0498	27.5	6.2	8.6	135	0.94, 0.95
0598	25.5	4.8	8.7	97	0.93, 0.93

a. measured at the origin of the anatomical coordinate system

b. ρ_0 = cross correlation between array prediction and reference reading at zero delay.
ρ_{max} = maximum cross correlation between array prediction and reference reading.

Table 3: Relative pressure measurements in the experiments[a]

Experiment	Fracture	Maximum near side pressure (KPa)	Minimum near side pressure (KPa)	Maximum far side pressure (KPa)	Minimum far side pressure (KPa)
0697	depressed	32	-26	41	-23.2.
0797	depressed[c]	>115[b]	-75	>115[b]	-29
0897	linear	>690[b]	-46	138	-100
0997	depressed[c]	>1150[b]	-65	695	-23
1097	depressed[c]	341	-26	>350[b]	-24
0198	depressed	552	-38	150	-75
0298	mild depressed	20	-96	196	-89
0398	none	69	-66	31	-61
0498	linear	43	-43	103	-91
0598	none	78	-44	104	-91

a. Pressure measurements are quoted relative to atmospheric pressure (1 atm = 0)
b. over range
c. comminuted

FINITE ELEMENT MODEL

MODELLING PHILOSOPHY - The purpose of the finite element model was to predict the mechanics of the impact in the brain tissue. The model considers the skull as a container that transmits loads to the brain. The model is designed so that kinematics are directly applied to the skull as well as impact loads. It was clear from dynamic data collected in these experiments that the entire head does not act as a rigid and free body during impact and that loads transmitted to the skull from non-rigid components of the head affect the kinematic results. For the purposes of the model we have assumed that the skull may be approximated as rigid in regions that are immediately adjacent to the brain but that are remote from the impact site. We have assumed that the kinematics of this rigid region of the skull may be described by the kinematics measured by the accelerometer array that was mounted to the skull of the animal. The skull is modelled as deformable in the region of impact to allow transmission of contact loads to the brain. The model of the brain includes the left and right hemispheres partitioned from the cerebellum by the tentorium.

MESH GENERATION - One of the experimental animals was sacrificed to collect geometrical data for the mesh generation and the post processing of finite element model results. MRI images of an intact and freshly killed sheep were taken at 1 mm intervals over the volume of the head. The head was immediately removed, frozen and CT scanned over the same volume. The head was then partially dissected for direct measurements of the dural membranes.

The CT data was used to define the interior and exterior surfaces of the skull. Surfaces were extracted using a nodal projection technique within the software package Persona (Abbott and Netherway, 1991). These surfaces were exported to a 3D modelling package Amapi (Template Graphics Software, Inc.) where extra construction surfaces were defined in preparation for mesh generation. The mesh itself was generated in ANSYS and exported to LSDYNA. The tentorium and falx were modelled by making direct contour measurements of the frozen head with the three dimensional digitiser in Amapi and then by exporting the surfaces to ANSYS for final mesh generation. The CT data and the direct measurement data were aligned by using anatomical landmarks which were identifiable in the CT data and measured on the actual skull at the time that the dura was modelled.

Using the same landmarks, the coordinate transformation between the MRI and the CT data was defined. This allowed CT coordinate data (and hence finite element coordinate data) to be readily related to the anatomical detail visible in the MRI data.

The model consists of 1024 elements that represent the impact region of the skull, 1280 elements for the rigid body part of the skull, 2912 elements for the brain and 271 elements for the tentorium and falx (which is very small in the sheep). The model is illustrated in Figure 4.

MATERIAL PROPERTIES, BOUNDARY CONDITIONS AND FINITE ELEMENT MODEL VALIDATION

Published material properties for the tissues of the brain vary widely and satisfactory definitions of the brain/skull interface have yet to be demonstrated. Previous finite element models have either modelled the behaviour of brain tissue as linear elastic or as viscoelastic. These material characterisations have largely been based on work done some twenty five years ago (McElhaney et al., 1973; Shuck and Advani, 1972). More recently Mendis et al. (1995), characterised the behaviour of brain tissue by the strain energy density function of a hyperelastic material. They were able to model the behaviour of a sample of brain tissue over a range of loading conditions, including large

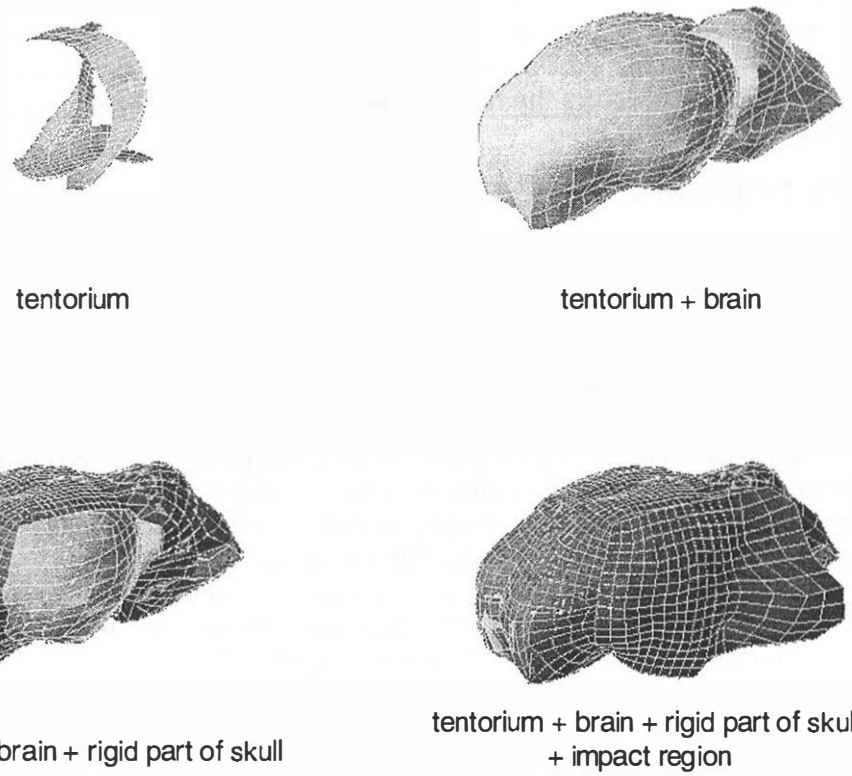

FIGURE 4. Finite element model

strains. Other work shows that regional differences exist in the brain's material properties. Arbogast and Margulies (1998) demonstrated that brain tissue in the brainstem is stiffer than that of the cerebral hemispheres and that the tissue exhibits anisotropic behaviour. We plan to incorporate some of these recent findings in our finite element model. However, as a first order of approximation, we have used a linear elastic model to describe the material properties of the brain. Claessens et al. (1997) showed that for short duration events and for certain viscoelastic characterisations, viscoelastic models gave very similar pressure results to a model that used a linear elastic characterisation. Table 4 lists the material properties used in the model.

Table 4: Material properties assigned to the finite element model

	Density (kg/m^3)	Young's modulus (Pa)	Poisson's ratio	Reference
skull	3000	6.5×10^9	0.22	Claessens (1997)
brain	1040	1.0×10^5	0.48	Claessens (1997)
tentorium	1130	3.15×10^7	0.45	Ruan et al. (1997)

In preliminary simulations, the boundary between the skull and the brain was modelled as fixed, and then as a simple contact that allowed separation and sliding. Some researchers have encountered problems when trying to define a realistic interface between the skull and the brain. The definition of a slip condition between the skull and

the brain can lead to problems with the two surfaces separating when the pressure at the interface reaches zero. The result of this is that these models do not represent the negative relative pressure behaviour seen in head impact experiments (see Claessens, 1997, and Miller et al., 1998 for recent examples). Our model also displayed this characteristic when the skull/brain interface was defined as a simple contact with sliding and separation. To capture the negative relative pressure behaviour, we fixed the brain nodes to the skull.

MODEL PERFORMANCE

Three experiments were selected for investigation using the finite element model. They were experiments 0398, 0498 and 0598. Experiment 0398 and 0598 were free from fractures and the animal in Experiment 0498 received a small linear fracture without tissue disruption or comminution. The experimentally recorded force and acceleration were applied to the model, and tracer particles were defined to measure the pressure at equivalent locations to those chosen in each experiment.

PRESSURE RESULTS - Figure 5 shows the pressures predicted by the model compared to that measured in each experiment. The model pressure histories are of similar magnitude to the experimental pressures. In the experiments, peaks of positive pressure were sometimes seen on the far side at the beginning of the impact. The model does not predict these peaks. A possible reason for this could be a rapid volume change in the skull; this change cannot be represented in the current finite element model because most of the skull is represented as a rigid entity.

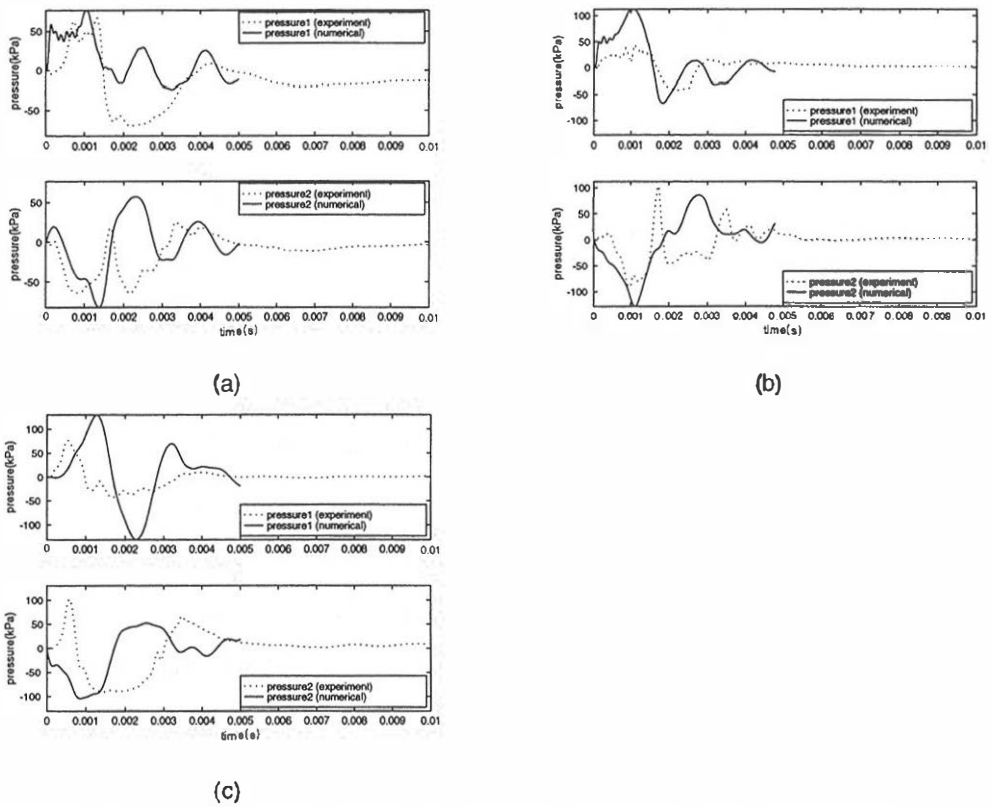

FIGURE 5. Pressures predicted by the finite element model and those recorded in Experiment 0398 (a), Experiment 0498 (b) and Experiment 0598 (c). Pressure 1 is the pressure measured on the near side and pressure 2 is that measured on the side further from the impact point.

MECHANICAL RESPONSE TO IMPACT - The model was examined at three coronal cross-sectional locations; one in the anterior region of the brain, one medial and one posterior in the occipital region of the brain. Each section was offset from the next by 10 mm. The cross-sections were chosen to match histology sections that had been examined for the presence of axonal injury. The location and orientation of the cross-section plane was found by matching the image of an oblique cut through the MRI data to the histology section. The equation of the plane was transformed to finite element coordinates and any element in the model cut by the plane was selected. This set of elements was interrogated further; the time histories of these elements were extracted from the finite element results and the maximum values of pressure, von Mises' stress, first principal stress, maximum shear stress, first principal strain and maximum principal shear strain were recorded for each element. Contour plots were generated on the basis of these maxima and compared to the results of the histology.

MODEL PREDICTIONS

GENERAL CHARACTERISTICS - Peak pressures were generally seen under the impact location and on the side furthest from impact. Peak negative pressures were always seen in the *contrecoup* region. Peak pressures were around 100 kPa in the *contrecoup* regions of the brain and up to 170 kPa in the *coup* region of the brain, while negative pressures reached -140 kPa in the *contrecoup* region. These results are similar to those relative pressures measured in the non-fracture experiments, except for negative relative pressures, which were limited in the experiments to around -100 kPa (vaporisation pressure). The distribution of peak values were similar for von Mises' stress, first principal strain, maximum shear stress and maximum shear strain. High values were seen in elements near the tentorium, and in the central part of the brain, in elements representing the left occipital lobe and in elements representing the parietal lobe. The distribution of peak values of first principal stress was somewhat different, with the highest regions of stress existing around the impact region and in the periphery of the brain generally.

MODEL PREDICTIONS AND OBSERVED INJURY - Figure 6 compares the output of the model to the observed injury distribution in two example sections. The contours are of von Mises' stress and the injury distribution is of 1+ and 2+ injury. These two examples are typical in that there are similarities between regions of high von Mises' stress and the incidence of 2+ injury within each slice. In the posterior section, the model predicts high von Mises' stresses in the elements along the margins of the tentorium and in the left hemisphere generally, particularly in the superior region. We commonly observed injury in these regions, although in non-fracture cases, injury was bilateral and not necessarily more pronounced in the left hemisphere. In the medial section, injury was consistently concentrated in the central region of the brain; the model predicted the highest von Mises' stress in the central region, although in regions that were superior to those found to have the most intense injury. The anterior section was consistently less severely injured, and the model also predicted much lower stresses in this region.

Although there appears to be some consistency between areas of higher von Mises' stress and regions of injury in particular sections, when sections within the same brain are compared, similarities were not as strong. In general, the model predicted the highest von Mises' stress in the posterior regions of the brain, but these regions were not necessarily more severely injured than other regions. Stresses which seemed to relate to 2+ injury in the medial section did not relate to the same severity of injury in the anterior section.

To explore this further, an analysis was performed to see if there was any relationship between the amount of injury observed in the brain and the proportion of the

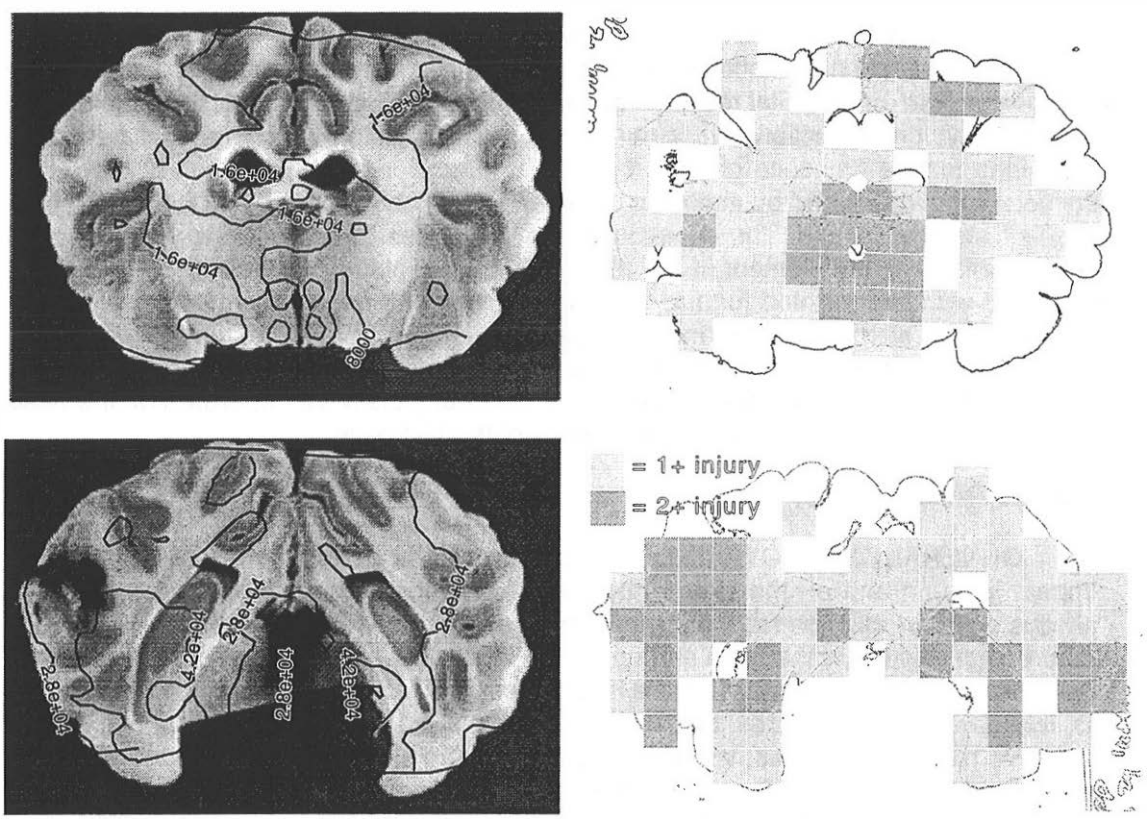

FIGURE 6. Contours of maximum von Mises' stress (Pa) predicted by the finite element simulation in the medial section in Experiment 0398 (top left) and map of injury distribution (top right) and at the posterior section in Experiment 0498 (lower left) and map of injury distribution (lower right). Note that the brain stem is not included in the image of the brain slice, but is included in the model.

model that experienced high von Mises' stress. Figure 7 plots the proportion of grid squares scoring an injury level of 2+ or greater against the proportion of the elements in the section that experienced a von Mises' stress of more than 30 kPa. There seems to be a trend of increasing injury with predicted stress, although the relationship just fails to be statistically significant at the 0.05 level ($R(7) = 0.629$, $p > 0.05$, $R^2 = 0.3954$).

DISCUSSION

The finite element model presented here is intended for use as a tool for preliminary investigation of the tissue mechanics during the impact with the head of the experimental animal. Simplified representations have been used for the material properties of the brain and the interface conditions between structures of the head. The only internal structure that has been included is the division between the cerebral hemispheres and the cerebellum by the tentorium. Although there is a suggestion from the data that the output of the finite element model may relate to injury observed in the animal model, such a relationship is not significantly apparent from the analyses performed thus far. On the basis of the distribution of injury, the model seems to overestimate the level of stress near the interface between the skull and the brain, relative to the rest of the model. This is apparent from the high levels of von Mises' stress predicted in the occipital lobe. This region of the model is constrained along its margins to the skull and the tentorium, possibly creating higher shear stresses than those predicted for regions deeper inside the brain. A more realistic interface between the brain

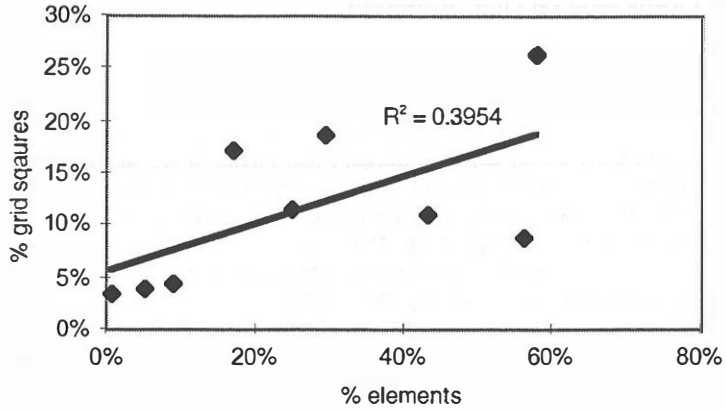

FIGURE 7. Plot of the proportion of each slice with an injury of 2+ or more against the proportion of each section predicted to have a maximum von Mises' stress of > 30 kPa

and the skull may improve this part of the model. Similarly, the model does not include the fissure between the hemispheres, nor the lateral ventricles, and these structures are likely to influence the distribution of stress in the model.

SUMMARY

The animal model of injury presented here has now progressed to a stage where we are able to measure the head kinematics during impact using an extension of the 3-2-2-2 accelerometer concept, which includes a reference accelerometer, that provides a means of validating acceleration measurements *in situ.* Additional accuracy is gained by the use of coordinate data throughout every stage of the study; three-dimensional coordinate data recorded in the experimental setting makes the accurate application of loads to the finite element model possible. Similarly, coupled coordinate data allow the extraction of finite element results in planes for which we have histological data.

In the animal model itself, a spectrum of injury is apparent after 4 hours survival. Axonal injury is more intense under the site of impact when the skull of the animal fractures.

The biomechanical data recorded in the experiments are being used to study the tissue mechanics during impact by applying them to a finite element model of the impact. The model presented in this paper is preliminary, and planned enhancements include more realistic material properties, the inclusion of a fluid layer between the skull and brain and better anatomical definition within the model. Other future work will include the simulation of as many sheep experiments as possible, using the methodology outlined in this paper.

It may be possible to relate the presence of injury in the brain to the predictions of the finite element model on a region by region basis, rather than over a whole slice, as presented in this paper. If so, it should be possible to determine a tissue level threshold of stress or strain, above which injury is likely to occur. Such an injury threshold may be useful as a threshold for injury in the analysis of human head impact.

ACKNOWLEDGEMENTS

This project was funded through a Unit grant from the National Health and Medical Research Council. The authors wish to thank staff from the Animal Care Services at the Institute of Medical and Veterinary Science, the Departments of Radiology at the Royal

Adelaide Hospital and at the Women's and Children's Hospital, and Dr. David Netherway of the Australian Cranio-Facial Unit, Adelaide.

REFERENCES

Abbott, A. and Netherway, D. 1991, 'Persona', Institute of Cranio-Facial Studies, Adelaide, South Australia.

Anderson, R.W.G., Brown, C.J., Scott, G., Blumbergs, P.C., Finnie, J.W., McLean, A.J. and Jones, N.R. 1997, 'Biomechanics of a sheep model of axonal injury', *1997 International IRCOBI Conference on the Biomechaincs of Impact, Hannover (Germany), 24-26 September 1997*, International Research Council on the Biomechaincs of Impact, pp. 181-192.

Arbogast, K.B. and Margulies, S.S. 1998, 'Material characterisation of the brainstem from oscillatory shear tests', *Journal of Biomechanics*, vol. 31, pp. 801 - 807.

Claessens, M.H.A. 1997, *Finite Element Modeling of the Human Head under Impact Conditions*, Mechanical Engineering, Technical University of Eindhoven, Eindhoven, Netherlands, 137 pages.

Gentleman, S.M., Nash, M.J., Sweeting, C.J., Graham, D.I. and Roberts, G.W. 1993, 'B-Amyloid precursor protein (BAPP) as a marker for axonal injury after head injury', *Neuroscience Letters*, vol. 160, pp. 139-144.

McElhaney, J.H., Melvin, J.W., Roberts, V.L. and Portnoy, H.D. 1973, 'Dynamic characteristics of the tissues of the head', Perspectives in Biomedical Engineering, University of Strathclyde, Glasgow, Scotland, June 1972, Ed, R.M. Kenedi, MacMillan Press Ltd., pp. 215-222.

Mendis, K.K., Stalnaker, R.L. and Advani, S.H. 1995, 'A constitutive relationship for large deformation finite element modeling of brain tissue', *Journal of Biomechanical Engineering*, vol. 117, no. 3, pp. 279-285.

Miller, R.T., Margulies, S.S., Leoni, M., Nonaka, M., Chen, X., Smith, D.H. and Meaney, D.F. 1998, 'Finite element modelling approaches for predicting injury in an experimental model for severe diffuse axonal injury', *42nd Stapp Car Crash Conference, Tempe, Arizona, USA*, Paper 983154, Society of Automotive Engineers, pp. 155-167.

National Health and Medical Research Council 1997, Australian code of practice for the care and use of animals for scientific purposes, Australian Government Publishing Service, Canberra.

Padgaonkar, A.J., Krieger, K.W. and King, A.I. 1975, 'Measurement of angular acceleration of a rigid body using linear accelerometers', *Journal of Applied Mechanics*, pp. 552-556.

Plank, G., Weinstock, H., Coltman, M. and Lee, H. 1989, 'Methodology for the Calibration and Data Acquisition with a Six-Degree-of-Freedom Acceleration Measuring Device', Report no. DOT-HS-807-370, National Highway Traffic Safety Administration, U.S. Department of Transportation, Washington DC, USA.

Ruan, J.S., Khalil, T.B. and King, A.I. 1997, 'Impact head injury analysis using an explicit finite element human head model', Journal of Traffic Medicine, vol. 25, no. 1-2, pp. 33-40.

Shuck, L.Z. and Advani, S.H. 1972, 'Rheological response of human brain tissue in shear', Journal of basic engineering, vol. 94, no. 4, pp. 905-911.